

Original Research

Spleen R2 and R2* in Iron-Overloaded Patients With Sick Cell Disease and Thalassemia Major

Casey J. Brewer, BS,^{1,2} Thomas D. Coates, MD,³ and John C. Wood, MD^{1,2*}

Purpose: To evaluate the magnetic properties of the spleen in chronically transfused, iron-overloaded patients with sickle cell disease (SCD) and thalassemia major (TM) and to compare splenic iron burdens to those in the liver, heart, pancreas, and kidneys.

Materials and Methods: A retrospective analysis of 63 TM and 46 SCD patients was performed. Spleen R2 and R2* values were calculated from spin-echo and gradient-echo images collected between April 2004 and September 2007.

Results: The spleen showed a different R2–R2* relationship than that previously established for the liver. At high iron concentrations (R2* > 300 Hz), spleen R2 was lower than predicted for liver. The proportion of splenic to hepatic iron content was greater in SCD patients compared with TM patients (23.8% vs. 13.8%). A weak association was found between splenic and liver iron—this association was stronger in SCD patients. Little correlation was found between splenic iron and extrahepatic R2* values.

Conclusion: For spleen and liver tissue with the same R2* value, splenic R2 was significantly lower than hepatic R2, particularly for R2* > ≈300 Hz. Splenic iron levels have little predictive value for R2* values of heart, pancreas, and kidney.

Key Words: spleen; sickle cell; thalassemia; MRI; iron
J. Magn. Reson. Imaging 2009;29:357–364.
 © 2009 Wiley-Liss, Inc.

PATIENTS WITH THALASSEMIA MAJOR (TM) are dependent on blood transfusions for survival (1). Approx-

imately 20% of sickle cell disease (SCD) patients, such as those with prior neurovascular events or abnormal transcranial Doppler examinations, also receive chronic transfusion therapy to prevent further vascular sequelae (2). However, routine transfusion therapy causes these patients to receive roughly 0.4 mg/kg/day of heme iron, which is over 25 times the physiological rate of iron absorption (2). Left untreated, iron overload can cause lethal endocrine and cardiac complications in the second decade of life (3). Chelation therapy is required as a preventative measure, and a close monitoring of iron levels is necessary to ensure proper treatment. Magnetic resonance imaging (MRI) has emerged as a noninvasive and accurate method of estimating the iron concentrations of the body's organs, including the liver, pancreas, heart, and kidneys (4–8).

The spleen is the second largest iron depot of the body after the liver (9). However, little is known about its magnetic properties or the role it plays in the body with respect to iron overload. The scale of iron storage (ie, size of iron particle aggregates) is larger in the spleen than in the liver due to clustering of iron-filled reticuloendothelial cells (10)—this could in turn affect the estimation of splenic iron concentration by MRI (11). We hypothesized that the larger iron scale in the spleen would cause R2 techniques to be less sensitive to iron in the spleen than in the liver, while R2* techniques would be relatively unaffected (11,12). We therefore compared the relationship between the two measurements in the spleen and in the liver in a cohort of TM and SCD patients.

Splenic iron regulation has not been well studied. It is known that hyperabsorption syndromes, such as thalassemia intermedia and hemochromatosis, spare the spleen relative to transfusional siderosis (13). However, one might expect variation among different types of transfusional siderosis as well (14). We hypothesized that splenic iron concentration would be higher in chronically transfused SCD patients because of insidious splenic volume loss, but that total splenic iron content would be the same or lower than chronically transfused TM patients. We also explored what relationship, if any, could be found between splenic iron and the iron concentration of other organs such as the liver, pancreas, heart, and kidneys in these two diseases.

¹Division of Cardiology, Childrens Hospital Los Angeles, Keck School of Medicine, University of Southern California, Los Angeles, California.

²Department of Radiology, Childrens Hospital Los Angeles, Keck School of Medicine, University of Southern California, Los Angeles, California.

³Division of Hematology-Oncology, Childrens Hospital Los Angeles, Keck School of Medicine, University of Southern California, Los Angeles, California.

Contract grant sponsor: National Heart, Lung, and Blood Institute (NHLBI); Contract grant number: 1 RO1 HL075592-01A1; Contract grant sponsor: General Clinical Research Center at Childrens Hospital Los Angeles; Contract grant number: RR000043-43; Contract grant sponsor: Center for Disease Control; Contract grant number: Thalassemia Center Grant U27/CCU922106; Contract grant sponsor: Novartis Pharma.

*Address reprint requests to: J.W., CHLA, Cardiology #34, Los Angeles, CA 90027. E-mail: jwood@chla.usc.edu

Received July 8, 2008; Accepted October 29, 2008.

DOI 10.1002/jmri.21666

Published online in Wiley InterScience (www.interscience.wiley.com).

MATERIALS AND METHODS

Study Group

We retrospectively examined the MR images of 103 chronically transfused TM patients (2.0–47.3-year-olds) and 92 chronically transfused SCD patients (1.6–31.7-year-olds) for splenic iron overload. The most recent exam for each patient was used when possible. All of the MR exams used in this study were performed between the dates of April 2004 and September 2007 for clinical evaluation of iron overload. Waiver of informed consent was approved by the Institutional Review Board. Both patient groups received transfusions at 3-week intervals to maintain pretransfusion hemoglobin between 9 and 10 g/dL. All patients were on iron chelation therapy with deferasirox or deferoxamine.

MRI and Interpretation

MRI of liver, heart, pancreas, and kidneys is routinely done for clinical care purposes at our institution. Examinations were performed on a 1.5T General Electric (Milwaukee, WI) CVi scanner running system 9.1. Liver and spleen volume were estimated by direct planimetry from a breath-hold 32 slice 3D steady-state free precession acquisition of the abdomen (MASS 4.0 software, MEDIS, The Netherlands). Liver R2* was measured during a single breath-hold from a single mid-hepatic slice using a single echo, gradient echo sequence; echo time (TE) was automatically incremented 15 times at logarithmic intervals from 1–16 msec. Other imaging parameters included a field of view (FOV) of 48 × 24 cm, a flip angle of 20°, a repetition time (TR) of 25 msec, a matrix of 64 × 64, a slice thickness of 10 mm, and a bandwidth of 83 kHz. Liver R2 was measured from four slices using a single echo, 90°–90° Hahn echo, using TEs of 3, 3.5, 5, 8, 12, 18, and 30 msec. Other imaging parameters included an FOV of 48 × 24 cm, a TR of 300 msec, a matrix of 64 × 64, a slice thickness of 10 mm, a gap of 5 mm, and a bandwidth of 32 kHz. Spleen R2 and R2* values were calculated from the same spin-echo and gradient-echo images. Heart, pancreas, and kidney R2* were estimated by using a multiecho-gradient echo T2* sequence having the following parameters: FOV 32–40 cm and a 75%–100% phase FOV, slice thickness 5–8 mm, flip 20°, matrix 128 × 128 (pancreas, kidney), matrix 192 × 256 (heart), and bandwidth 125 kHz. Eight equally spaced echoes were collected from 1.1–13.5 msec (pancreas, kidney) and from 2.2–17.6 msec (heart). Electrocardiographic or peripheral pulse gating was used for all cardiac imaging but not for any of the other acquisitions.

Relaxivities were calculated pixelwise to an exponential plus constant using custom MatLab (MathWorks, Natick, MA) routines (15). Regions of interest encompassed the entire liver, spleen, and kidney. Pancreas regions of interest avoided the pancreatic head because of susceptibility artifacts. Cardiac measurements were limited to the interventricular septum to avoid susceptibility artifacts from the great cardiac veins and air-tissue interfaces (8,15). Hepatic iron concentrations (HIC) were estimated from mean R2 and R2* values using previously published calibration curves (6,7). The

calibration curve describing the curvilinear relationship between R2 and HIC was derived by St Pierre et al: $R2 = 6.88 + 26.06[Fe]^{0.701} - 0.438[Fe]^{1.402}$ and confirmed by our laboratory (6,7). The linear relationship between R2* and liver iron can be expressed as follows: $[Fe]_{R2*} = 0.0254 \times R2* + 0.202$ (7).

Hepatic iron content (HC) was estimated using HIC (dry weight), liver volume (calculated at time of exam), and an assumed wet weight to dry weight ratio (WTDR) of 4.1 (16). Spleen iron concentration (SIC) was calculated using splenic R2* values only, assuming an R2* calibration similar to liver. Splenic iron content (SC) was estimated using the calculated SIC (dry weight), spleen volume, and a WTDR of 4.29. Human spleen WTDR has not been published, therefore we estimated it as follows: (human liver WTDR of 4.1) * (mouse spleen WTDR of 3.42)/(mouse liver WTDR of 3.27) (17). Splenic analysis was not possible in some patients because of splenic infarction or splenectomy.

Cardiac R2* values rise linearly with respect to cardiac iron in animal and autopsy studies. However, clinical correlations are typically made with respect to the relaxivity values, so we did not attempt to convert R2* values to cardiac iron concentration. Kidney R2* have not been calibrated to iron stores in either animal or human studies. In SCD, kidney R2* is dominated by cortical iron deposition from intravascular hemolysis. Kidney R2* values tend to be normal in TM (due to the lack of intravascular hemolysis) but mild elevations are observed in patients with severely elevated HIC.

Statistical Analysis

Univariate and multivariate regression was performed using JMP v. 5.1.2 (SAS, Cary, NC). Bonferroni correction was applied to compensate for multiple comparisons. Univariate correlations were considered significant if the *P*-value was less than 0.05 after Bonferroni correction. Forward stepwise multivariate analysis was subsequently performed upon all of the significant univariate terms. Terms were retained after multivariate analysis if the *P*-value was less than 0.05. Occasionally, HIC and/or SIC were excluded from multivariate analysis because they were redundant due to the presence of HC or SC, respectively.

RESULTS

Our retrospective analysis included 103 TM and 92 SCD patients. Surgical splenectomy had been performed in 56 patients (40 TM, 16 SCD), while 30 SCD patients had badly infarcted spleens (Fig. 1 demonstrates a representative normal and infarcted spleen). Final spleen analysis was therefore limited to 63 TM and 46 SCD patients.

Of the analyzable patients, SCD patients were younger than TM patients (11.6 ± 5.3 years vs. 16.4 ± 8.3 years, $P < 0.0002$), but well matched for gender (41% male vs. 54% male) and for HIC (14.0 ± 9.8 mg/g dry weight vs. 13.0 ± 12.5 mg/g dry weight, $P > 0.67$).

Prior work suggests that patients with SCD and TM have similar relaxivity-iron relationships in the liver (7); this was confirmed in Fig. 2A, demonstrating liver R2–

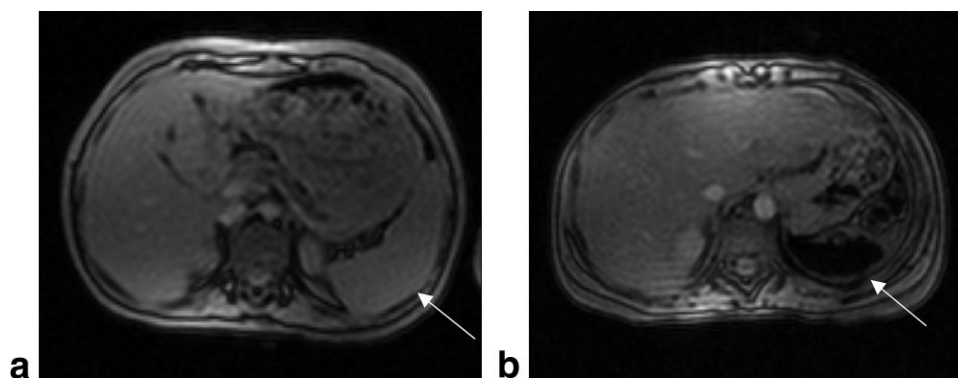


Figure 1. Example of (A) a normal spleen in a TM patient and (B) an infarcted spleen in an SCD patient. Because of iron concentration from volume loss, the iron levels of infarcted spleens were too high to be measured by MRI. Thirty SCD patients had infarcted spleens and thus had to be omitted from the present study.

R2* relationships for the two diseases. R2 has a curvilinear relationship with R2*, similar to its known relationship with liver iron (6,7), indicating a loss of sensitivity to iron at higher concentrations (18).

The corresponding R2–R2* relationship for spleen is demonstrated in Fig. 2B; the liver R2–R2* relationship is shown for reference (solid line). At low R2* levels ($R2^* < 200$ Hz), spleen had comparable R2–R2* behavior to liver, although there was greater variability. However, spleen R2 values were lower than predicted at higher iron concentrations ($R2^* > 300$ Hz, Fig. 2B). This decrease in R2-sensitivity to splenic iron was found in both SCD and TM patients. In general, patients with SCD displayed greater splenic iron concentrations, with R2* increasing as high as 1400 Hz. In all, there were 13/46 SCD patients with splenic R2* values above 600 Hz, while only 1/63 TM patients had a value this high ($P < 0.0001$ by Fischer's exact test).

Given the documented loss of R2 iron-sensitivity relative to R2* in these patients and prior work documenting the critical dependence of R2 on particle size (11,12,19), we used R2* alone to estimate SIC, assuming a calibration equal to liver. Since splenic volume loss could account for the increased splenic R2* seen in SCD patients (through a concentration effect), we compared estimated splenic and liver iron contents. A weak association was found in both SCD and TM (Fig. 3A). The association was found to be stronger in SCD (Table 1). In TM, splenic iron content plateaus at 1–1.5g even as hepatic content continued to grow. This quick saturation of splenic iron content was not seen in SCD. Instead, splenic iron continued to increase with hepatic iron in some SCD patients until spleen R2* values could no longer be measured ($R2^* > 1500$ Hz). The spleen to liver iron content ratio was $13.7\% \pm 18.2\%$ in TM vs. $23.8\% \pm 21.2\%$ in SCD patients ($P = 0.01$). Figure 3B

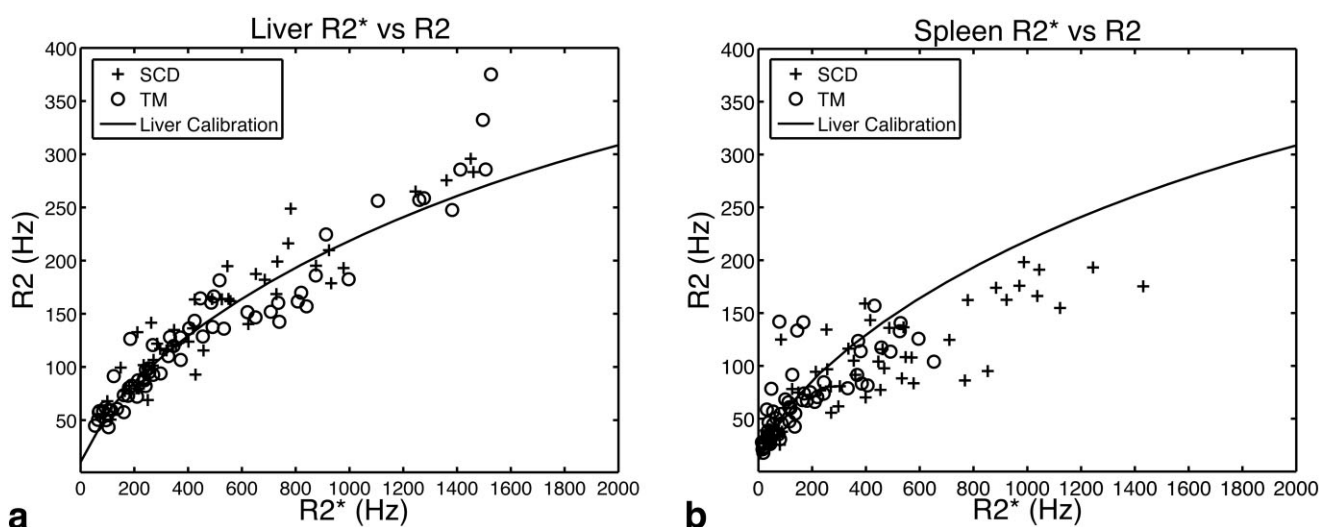


Figure 2. A: Relationship between hepatic R2 and R2* in SCD and TM (restricted to patients that had spleens analyzable by MRI). Individual points are compared with a previously determined liver calibration curve for hepatic R2 and R2* (7). Predicted HIC increases linearly with R2* and nonlinearly with R2, producing the curvilinear relationship between them. **B:** Spleen R2 vs. spleen R2* in SCD (+ symbols) and TM (open circles) patients. Solid line depicts the known R2–R2* calibration for liver. Compared to the liver calibration, spleen R2 begins to decline relative to R2* values once R2* exceeds around 300 Hz (7.8 mg/g dry weight of liver). All TM patients have spleen R2* < 650 Hz, while 13 SCD patients exceed this value.

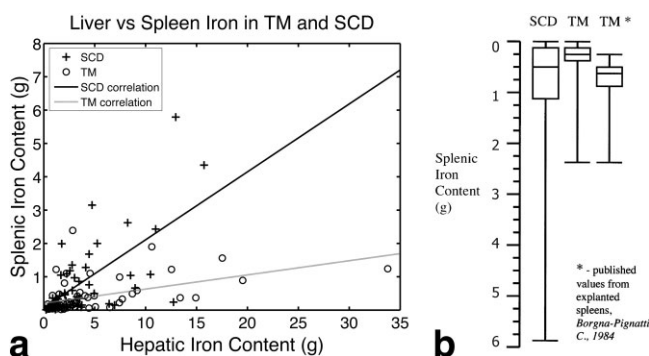


Figure 3. A: Relationship between hepatic iron content and splenic iron content in SCD and TM patients. Black line depicts relationship among SCD patients ($r^2 = 0.40$, $P < 0.0001$). Gray line depicts relationship among TM patients ($r^2 = 0.23$, $P < 0.0001$). **B:** Estimated splenic iron contents of SCD and TM patients from this study compared with biochemically determined splenic iron contents of splenectomized TM patients from a previously published study (20). The range of iron burden is nearly identical between the literature and the present study; the greater mean values observed in the splenectomized patients most likely reflects the clinical indication for splenectomy (hypersplenism).

compares estimated splenic iron contents against biochemically determined iron levels in explanted spleens from TM patients (20).

Liver and spleen volumes increase with somatic growth, so all values were indexed to body surface area. Spleen volume index (SVI) was correlated to liver volume index (LVI) in TM (Fig. 4A, $r^2 = 0.19$, $P < 0.0003$) but not SCD (Fig. 4B, $r^2 = 0.01$, $P < 0.254$). SVI was a stronger determinant of splenic iron content in SCD ($r^2 = 0.45$, $P < 0.0001$) (Table 1) compared with TM ($r^2 = 0.18$, $P < 0.0004$) and SVI did not correlate with splenic

iron concentration in either TM or SCD (Table 1). Similarly, LVI was more closely related to hepatic iron content than hepatic iron concentration (Table 1). LVI and hepatic iron content increased with age in SCD but not TM patients (Table 1).

To determine how splenic iron levels correlated with extrahepatic iron deposition, iron concentrations and contents were compared among the heart, pancreas, kidney, liver, and spleen (Table 2); $R2^*$ was used as a surrogate for iron concentration in the heart, pancreas, and kidney. In TM patients, splenic iron content was correlated with renal $R2^*$ ($r^2 = 0.26$, $P = 0.0001$). Cardiac $R2^*$ was weakly correlated with SIC ($r^2 = 0.18$, $P < 0.0003$) and splenic iron content ($r^2 = 0.17$, $P < 0.0005$) but these associations disappeared on multivariate analysis. SCD patients did not show any correlation between splenic iron levels and the iron levels of extrahepatic organs (Table 2).

The most striking interorgan statistical association was found between cardiac $R2^*$, pancreatic $R2^*$ ($r^2 = 0.60$, $P < 0.0001$), and hepatic iron content ($r^2 = 0.59$, $P < 0.0003$) in TM patients; multivariate analysis yielded a combined r^2 value of 0.73 (Table 2).

The effect of splenectomy on HIC, liver iron content, liver volume, and cardiac $R2^*$ was examined in SCD and TM. In TM, liver iron concentration (8.2 ± 8.2 mg/g vs. 13.0 ± 12.5 mg/g dry weight, $P < 0.05$) was lower in splenectomized patients, but cardiac $R2^*$ trended higher (88.9 ± 71.9 Hz vs. 62.6 ± 71.9 Hz, $P = 0.08$); hepatic contents were not statistically different. In splenectomized SCD patients there was a trend toward higher hepatic iron content (7.6 ± 7.1 g vs. 4.1 ± 3.7 g, $P = 0.08$), but no difference in cardiac $R2^*$. Splenectomized patients were significantly older for both SCD (19.9 ± 5.7 years vs. 13.8 ± 6.5 years, $P < 0.0001$) and TM (30.7 ± 8.8 years vs. 21.8 ± 10.9 years) patients.

Table 1
Correlations Between Splenic and Hepatic Iron

Thalassemia major patients								
	SC	HIC	SIC	LVI	SVI	Age	Multivariate equation	r^2
HC	0.23^a	—	0.17^b	0.39^a	0.02	0.09	HC = $3.48 \times SC + 0.013 \times LVI - 9.49$	0.46
SC	—	0.16^a	—	0.13	0.18^a	0.10^a	SC = $0.014 \times HIC + 0.001 \times SVI + 0.015 \times Age - 0.398$	0.36
HIC	—	—	0.23^a	0.16^a	-0.01	-0.01	HIC = $1.28 \times SIC + 0.019 \times LVI - 10.69$	0.33
SIC	—	—	—	0.01	-0.02	0.00	—	—
LVI	—	—	—	—	0.19	0.06	—	—
SVI	—	—	—	—	—	0.01	—	—
Sickle cell disease patients								
	SC	HIC	SIC	LVI	SVI	Age	Multivariate equation	r^2
HC	0.40^a	—	0.10	0.14	0.13	0.34^a	HC = $1.53 \times SC + 0.29 \times Age - 0.62$	0.53
SC	—	0.21^a	—	0.19^a	0.45^a	0.13	SC = $0.03 \times HIC + 0.002 \times LVI + 0.004 \times SVI - 2.63$	0.61
HIC	—	—	0.04	-0.02	0.11	0.06	—	—
SIC	—	—	—	0.13	-0.01	0.00	—	—
LVI	—	—	—	—	0.01	0.34	—	—
SVI	—	—	—	—	—	0.02	—	—

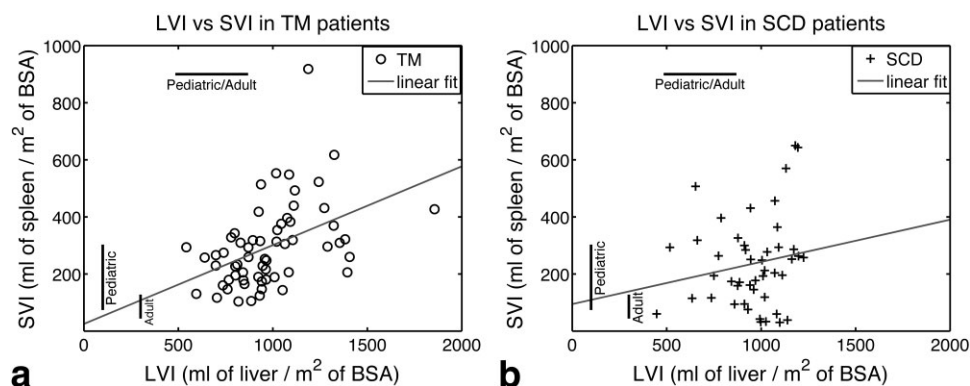
HC, hepatic iron content; SC, splenic iron content; HIC, hepatic iron concentration; SIC, splenic iron concentration; LVI, liver volume index; SVI, splenic volume index; r^2 , combined r^2 of terms retained after multivariate analysis.

Bold = significant at $P < 0.05$ after Bonferroni correction.

^aRetained after multivariate analysis, $P < 0.05$.

^bExcluded from multivariate analysis because redundant.

Figure 4. Relationship between liver volume index (indexed to body surface area), LVI, and spleen volume index, SVI, in (A) TM and (B) SCD. SVI rises proportionally to LVI in TM but not SCD. Solid lines indicate linear fits (TM: $r^2 = 0.19$, $P < 0.0002$ and SCD: $r^2 = 0.01$, $P < 0.254$).



DISCUSSION

R2 loses sensitivity to splenic iron at high concentrations, representing static refocusing from larger length scale of iron deposits (11,12,21). In hepatocytes, iron deposits have a mean diameter of $\approx 1 \mu\text{m}$ and are well tuned for R2 signal decay (22). Although iron deposits are of similar size in reticuloendothelial system (RES) cells, the interparticle distance is so small that the entire cell behaves as one large paramagnetic bead, having an effective diameter of 15–20 μm (10,22). Magnetically, fully saturated RES cells will have large length scale magnetic disturbances, causing static refocusing in spin echo experiments and lower R2 values at high iron concentrations (11,12,18). R2* techniques remain linearly proportional to iron in this scenario (11). While the liver has iron deposits in parenchymal tissue in addition to the RES, splenic iron deposition is confined to the RES (10). Thus, for spleen and liver tissue with the same R2* value, splenic R2 was expected to be significantly lower than hepatic R2. This was found to be true in both SCD and TM patients (Fig. 2B); however, this effect was seen only once R2* values had risen above $\approx 300 \text{ Hz}$ (Fig. 2B), likely reflecting a critical iron particle size/density where static refocusing starts to dominate.

The spleen is an integral part of iron recycling and conservation. The spleen stores are relatively less important in TM, having only 13.8% of hepatic iron burdens in TM and 23.8% in SCD. In TM patients, spleen iron appeared to saturate at relatively low hepatic iron concentration ($\approx 7 \text{ mg/g}$) relative to SCD patients (23), making this depot relatively more important at lower iron concentrations. One possible explanation for the disparity in loading is that the rigid sickle red blood cells more easily lodge in splenic vascular and sinusoidal spaces. Chronically transfused sickle cell disease patients still have almost one-third the circulating hemoglobin S red blood cells of nontransfused SCD patients, incompletely palliating the microvascular occlusive process (2). A second possible explanation is that SCD patients have greater inflammation, potentially locking iron in the splenic and hepatic RES (24,25).

One limitation of our study is that more than 40% of SCD and TM patients had either undergone surgical splenectomy or had severely infarcted spleens, introducing uncorrectable selection bias. Splenectomized patients with TM showed decreased HIC. Splenectomy is normally performed in TM patients with hypersplenism to reduce transfusion requirements. Despite the lower liver iron burden, splenectomized TM patients

Table 2
Correlations Between Splenic and Extrahepatic Iron

Thalassemia major patients									
	R2*P	R2*K	HC	HIC	SC	SIC	Age	Multivariate equation	R ²
R2*H	0.60^a	0.04	0.59^a	0.36^b	0.17	0.18^b	0.09	R2*H = .11×R2*P + 5.93×HC + 13.5	0.73
R2*P	—	−0.01	0.40^a	0.27^b	0.08	0.11	0.18^a	R2*P = 29.42×HC + 9.85×Age − 82.8	0.45
R2*K	—	—	0.01	0.00	0.26	0.08	−0.02	—	—
Sickle cell disease patients									
	R2*P	R2*K	HC	HIC	SC	SIC	Age	Multivariate equation	r ²
R2*H	0.15	0.01	−0.02	0.00	−0.02	0.00	−0.02	—	—
R2*P	—	−0.01	−0.01	−0.01	−0.02	−0.02	−0.02	—	—
R2*K	—	—	0.01	0.18	0.12	0.03	−0.01	—	—

R2*H, heart R2*, R2*P, pancreas R2*, R2*K, kidney R2*, HC, hepatic iron content, SC, splenic iron content, HIC, hepatic iron concentration, SIC, splenic iron concentration, r², combined r² of terms retained after multivariate analysis

Bold = significant at $P < 0.05$ after Bonferroni correction.

^aRetained after multivariate analysis, $P < 0.05$.

^bExcluded from multivariate analysis because redundant.

had a trend toward greater cardiac iron ($P = 0.07$). The mechanisms of this disparity are unclear but may reflect decreased extrahepatic iron buffering capacity in splenectomized patients. In contrast, splenectomized SCD patients displayed trends toward *increased* HIC and content. Splenectomy is performed for different indications in SCD patients, often in early childhood (prior to initiating transfusion therapy) in response to a splenic sequestration crisis. Thus, splenectomy is a marker for more severe vaso-occlusive disease and correlates with duration of transfusion therapy (12). Splenectomized patients (both TM and SCD) were significantly older than unsplenectomized patients and this difference may entirely explain observed differences in organ iron loading; one would need a more closely matched patient pool to address this question.

We postulated that liver and splenic volumes would increase proportionally to organ iron concentration as a compensatory response to iron toxicity. In fact, interactions between iron concentrations and organ volumes were quite weak. LVI fluctuations were associated with HIC only in TM patients; this may indicate greater relative hepatic iron toxicity in TM. SVI fluctuations were uncorrelated with SIC in both SCD and TM. SVI correlated with LVI in TM patients but not SCD patients (Fig. 4). One possible explanation for these disease-specific disparities is that extramedullary hemopoiesis is significantly greater in TM patients and could potentially expand splenic and hepatic RES simultaneously, independent of iron concentration; this would strengthen the correlation between LVI and SVI in TM. Alternatively, variations in splenic volume for SCD patients may be governed primarily by microvascular occlusion and splenic volume loss, destroying the association between LVI and SVI in SCD patients and strengthening the association between SVI and SC. Hepatosplenomegaly is common in the SCD and TM patients. However, comparing our observed SVI and LVI to population norms was confounded by the young age of our study population (our oldest patient with analyzable spleen was 31.6 years of age). Children have much larger spleens than adults and spleen volume decreases slowly throughout adulthood (26,27). Liver volume does not have as strong an age dependence, but significant ethnic differences have been observed (28).

The statistical association between splenic and hepatic iron concentrations and content were both relatively weak, reflecting independent modulating factors. Splenic iron content and concentration were also found to have little predictive value for extrahepatic iron deposition, suggesting that splenic iron levels are relatively independent of nontransferrin-bound iron levels.

One unexpected but novel finding of our analysis was that cardiac iron ($R2^*$) was more strongly associated with liver iron content ($r^2 = 0.59$) than with HIC ($r^2 = 0.36$) in TM (Table 2). In fact, liver iron content was a better predictor of extrahepatic organ iron accumulation ($R2^*$) for the majority of the organs, suggesting that concomitant measurement of liver volume has clinical utility. This approach has been previously advocated by some practitioners of SQUID liver iron analysis (9). The

combined r^2 of cardiac $R2^*$, liver iron content, and pancreatic iron in TM was 0.73, suggesting that an abdominal iron assessment might be a reasonable screening tool for the presence of cardiac iron. This observation warrants prospective clinical evaluation.

Prior work investigating splenic iron by MR predominantly reported spleen intensity ratios using either gradient or spin-echo sequences (13,29–32). This method can be used to demonstrate differential loading of the spleen relative to other organs but is not quantitative. In general, splenic iron loading is greater in transfusional siderosis compared with genetic hemochromatosis (13,30), consistent with the reticuloendothelial composition of the spleen. Although others have noted heavy splenic iron deposits in transfused SCD patients, our study is the first to systematically demonstrate greater splenic iron burdens relative to TM patients. Spleen relaxometry has been thus far limited to $R2$ analysis (33,34); our study is the first reported $R2^*$ data. However, as demonstrated in this article, $R2$ analysis probably underestimates splenic iron, although *ex vivo* validation of this principal will be necessary.

Observations in this article are confined to chronically transfused patients with SCD and TM. Splenic phenotypes would be quite different in nontransfused thalassemia and SCD patients. In nontransfused SCD, microvascular occlusion, erythrocyte sequestration and splenic infarction are the major sources of splenic iron overload, but they are accompanied by severe volume loss and calcification (35). Erythropoiesis is essentially normal and nontransfused SCD patients do not spontaneously load iron (2). In contrast, nontransfused thalassemia patients have markedly increased erythropoietic drive, low hepcidin levels, and increased iron absorption (36). The spleen is massively enlarged but not iron-loaded because of the lack of transfusions and because low hepcidin levels favor iron mobilization from reticuloendothelial stores (36).

Chronic transfusion therapy partially normalizes many of the disparities between the diseases. In SCD patients, chronic transfusion therapy lowers the percent sickle hemoglobin to below 30%, dramatically decreasing intravascular hemolysis, splenic infarction, and the classic SCD vascular phenotypes associated with hemolysis nitric oxide dysregulation (2,37). The earlier the onset of and the longer the duration of chronic transfusion therapy, the more a SCD patient would be expected to have a splenic phenotype resembling TM. In TM patients, chronic transfusion therapy normalizes ineffective erythropoiesis, decreasing spleen size, but producing splenic iron loading (2).

The primary limitation of this study is the assumption that the spleen $R2^*$ -iron calibration is the same as for liver; we do not have independent validation of this hypothesis. Nonetheless, $R2^*$ measurements are distributionally robust, depending primarily on magnetic susceptibility (11,21). Iron susceptibility is similar in spleen and liver, albeit slightly higher in nontransfusional siderosis (38,39). Our predicted spleen iron contents were consistent with published values from explanted spleens (Fig. 3B) (20). While it would be desirable to validate our predictions in patients scheduled for clinical splenectomies, we rarely perform this procedure any more because of

postsplenectomy thrombotic complications and pulmonary hypertension (40). However, any errors in the splenic iron calibration curve are likely to be simple slope adjustments that would have no effect on our correlation analysis and would not change the fundamental conclusions of the article.

Our splenic WTDR is a similar limitation. Knowledge of WDTR is essential for calibrating liver MRI measurements (which are sensitive to wet-weight iron concentration) to biopsy results (which are typically reported per gram of dry tissue). Since WTDR varies significantly with tissue processing, there is no universal agreement on liver WTDR; however, nonparaffin-embedded liver has a WTDR near 4.1. Since a splenic WTDR has yet to be published, we were forced to estimate human spleen WTDR based on human liver WTDR, mouse liver WTDR, and mouse spleen WTDR as described in Materials and Methods. Despite the ad-hoc nature of this approximation, our calculations of splenic iron content match up well with biochemical studies done on spleen explants (Fig. 3B) (20). Furthermore, errors in this parameter will not alter the correlation analysis or our fundamental conclusions.

In conclusion, R2 values are lower in spleen than in liver for a given R2* value at high iron concentrations, representing greater static refocusing from large iron deposits. Splenic iron rises proportionally to hepatic iron content at lower iron burdens but plateaus in TM near an HIC of 7–8 mg/g, consistent with the smaller capacity of RES stores. Patients with SCD develop greater splenic iron burdens, potentially reflecting increasing red cell sequestration and vaso-occlusion. Neither spleen iron concentration nor content was useful in predicting extrahepatic iron deposition.

ACKNOWLEDGMENT

The authors thank Leila Noetzli for assistance with figure and article preparation.

REFERENCES

- Pippard MJ. Iron overload and iron chelation therapy in thalassemia and sickle cell haemoglobinopathies. *Acta Haematol* 1987; 78:206–211.
- Vichinsky EP. Current issues with blood transfusions in sickle cell disease. *Semin Hematol* 2001;38:14–22.
- Zurlo MG, De Stefano P, Borgna-Pignatti C, et al. Survival and causes of death in thalassemia major. *Lancet* 1989;2:27–30.
- Au WY, Lam WW, Chu W, et al. A T2* magnetic resonance imaging study of pancreatic iron overload in thalassemia major. *Haematologica* 2008;93:116–119.
- Schein A, Enriquez C, Coates TD, Wood JC. Magnetic resonance detection of kidney iron deposition in sickle cell disease: a marker of chronic hemolysis. *J Magn Reson Imaging* 2008;28:698–704.
- St Pierre TG, Clark PR, Chua-anusorn W, et al. Noninvasive measurement and imaging of liver iron concentrations using proton magnetic resonance. *Blood* 2005;105:855–861.
- Wood JC, Enriquez C, Ghugre N, et al. MRI R2 and R2* mapping accurately estimates hepatic iron concentration in transfusion-dependent thalassemia and sickle cell disease patients. *Blood* 2005;106:1460–1465.
- Wood JC, Tyszka JM, Ghugre N, Carson S, Nelson MD, Coates TD. Myocardial iron loading in transfusion-dependent thalassemia and sickle-cell disease. *Blood* 2004;103:1934–1936.
- Fischer R, Tiemann CD, Engelhardt R, et al. Assessment of iron stores in children with transfusion siderosis by biomagnetic liver susceptibility. *Am J Hematol* 1999;60:289–299.
- Chua-anusorn W, Macey DJ, Webb J, de la Motte Hall P, St Pierre TG. Effects of prolonged iron loading in the rat using both parenteral and dietary routes. *Biomaterials* 1999;12:103–113.
- Tanimoto A, Oshio K, Suematsu M, Pouliquen D, Stark DD. Relaxation effects of clustered particles. *J Magn Reson Imaging* 2001;14: 72–77.
- Tanimoto A, Pouliquen D, Kreft BP, Stark DD. Effects of spatial distribution on proton relaxation enhancement by particulate iron oxide. *J Magn Reson Imaging* 1994;4:653–657.
- Siegelman ES, Mitchell DG, Rubin R, et al. Parenchymal versus reticuloendothelial iron overload in the liver: distinction with MR imaging [see Comments]. *Radiology* 1991;179:361–366.
- Siegelman ES, Outwater E, Hanau CA, et al. Abdominal iron distribution in sickle cell disease: MR findings in transfusion and nontransfusion dependent patients. *J Comput Assist Tomogr* 1994;18:63–67.
- Ghugre NR, Enriquez CM, Coates TD, Nelson MD Jr, Wood JC. Improved R2* measurements in myocardial iron overload. *J Magn Reson Imaging* 2006;23:9–16.
- Zuyderhoudt FM, Hengeveld P, van Gool J, Jorning GG. A method for measurement of liver iron fractions in needle biopsy specimens and some results in acute liver disease. *Clin Chim Acta* 1978;86:313–321.
- Nowak D, Pietras T, Antczak A, Krol M, Piasecka G. Effect of bacterial lipopolysaccharide on the content of lipid peroxidation products in lungs and other organs of mice. *Antonie Van Leeuwenhoek* 1993;63:77–83.
- Wood J, Aguilar M, Otto-Duessel M, Nick H, Nelson M, Moats R. Influence of iron chelation therapy on R1 and R2 calibration curves in gerbil liver and heart. *Magn Reson Med* 2008;60:82–89.
- Wood JC, Fassler J, Meade T. Mimicking liver iron overload using liposomal ferritin preparations. *Magn Reson Med* 2004;51:607–611.
- Borgna-Pignatti C, De Stefano P, Bongo IG, Avato F, Cazzola M. Spleen iron content is low in thalassemia. *Am J Pediatr Hematol Oncol* 1984;6:340–343.
- Weisskoff RM, Zuo CS, Boxerman JL, Rosen BR. Microscopic susceptibility variation and transverse relaxation: theory and experiment. *Magn Reson Med* 1994;31:601–610.
- Ghugre NR, Coates TD, Nelson MD, Wood JC. Mechanisms of tissue-iron relaxivity: nuclear magnetic resonance studies of human liver biopsy specimens. *Magn Reson Med* 2005;54:1185–1193.
- Harmatz P, Butensky E, Quirolo K, et al. Severity of iron overload in patients with sickle cell disease receiving chronic red blood cell transfusion therapy. *Blood* 2000;96:76–79.
- Papanikolaou G, Tzilianos M, Christakis JI, et al. Hepcidin in iron overload disorders. *Blood* 2005;105:4103–4105.
- Walter PB, Fung EB, Killilea DW, et al. Oxidative stress and inflammation in iron-overloaded patients with beta-thalassemia or sickle cell disease. *Br J Haematol* 2006;135:254–263.
- Schlesinger AE, Edgar KA, Boxer LA. Volume of the spleen in children as measured on CT scans: normal standards as a function of body weight. *AJR Am J Roentgenol* 1993;160:1107–1109.
- Kaneko J, Sugawara Y, Matsui Y, Makuuchi M. Spleen size of live donors for liver transplantation. *Surg Radiol Anat* 2008;30:515–518.
- Yoshizumi T, Taketomi A, Kayashima H, et al. Estimation of standard liver volume for Japanese adults. *Transplant Proc* 2008;40: 1456–1460.
- Emy P, Levin T, Sheth S, Ruzal-Shapiro C, Garvin J, Berdon W. Iron overload in reticuloendothelial systems of pediatric oncology patients who have undergone transfusions: MR observations. *AJR Am J Roentgenol* 1997;168:1011–1016.
- Yoon DY, Choi BI, Han JK, Han MC, Park MO, Suh SJ. MR findings of secondary hemochromatosis: transfusional vs erythropoietic. *J Comput Assist Tomogr* 1994;18:416–419.
- Arrive L, Thurnher S, Hricak H, Price DC. Magnetic resonance imaging of splenic iron overload. *Eur J Radiol* 1990;10:98–104.
- Papakonstantinou O, Drakonaki EE, Maris T, Vasiladou A, Papadakis A, Gourtsoyiannis N. MR imaging of spleen in beta-thalassemia major. *Abdom Imaging* 2006 (in press).
- Drakonaki EE, Maris TG, Papadakis A, Karantanas AH. Bone marrow changes in beta-thalassemia major: quantitative MR imaging findings and correlation with iron stores. *Eur Radiol* 2007;17:2079–2087.
- Gossuin Y, Muller RN, Gillis P, Bartel L. Relaxivities of human liver and spleen ferritin. *Magn Reson Imaging* 2005;23:1001–1004.
- Siegelman ES, Mitchell DG, Semelka RC. Abdominal iron deposition: metabolism, MR findings, and clinical importance. *Radiology* 1996;199:13–22.

36. Origa R, Galanello R, Ganz T, et al. Liver iron concentrations and urinary hepcidin in beta-thalassemia. *Haematologica* 2007;92:583–588.
37. Gladwin MT, Schechter AN. Nitric oxide therapy in sickle cell disease. *Semin Hematol* 2001;38:333–342.
38. St Pierre TG, Dickson DP, Kirkwood JK, Ward RJ, Peters TJ. A Mossbauer spectroscopic study of the form of iron in iron overload. *Biochim Biophys Acta* 1987;924:447–451.
39. St Pierre TG, Chua-anusorn W, Webb J, Macey D, Pootrakul P. The form of iron oxide deposits in thalassemic tissues varies between different groups of patients: a comparison between Thai beta-thalassemia/hemoglobin E patients and Australian beta-thalassemia patients. *Biochim Biophys Acta* 1998;1407:51–60.
40. Phrommintikul A, Sukonthasarn A, Kanjanavanit R, Nawarawong W. Splenectomy: a strong risk factor for pulmonary hypertension in patients with thalassaemia. *Heart* 2006;92:1467–1472.